33rd Annual International Conference of the IEEE EMBS
Boston, Massachusetts USA, August 30 - September 3, 2011

Spherical Harmonics based extraction and annotation of cell shape in 3D time-lapse microscopy sequences

Christel Ducroz, Jean-Christophe Olivo-Marin, *Senior Member, IEEE*, and Alexandre Dufour, *Member, IEEE*

***Abstract*— Understanding the mechanisms involved in cell deformation and motility is of major interest in numerous areas of life sciences. Precise quantification of cell shape requires robust shape description tools to be amenable to subsequent analysis and classification. The main difficulty lies in the great variability of cell shapes within a given homogeneous population. In this work, we propose a framework for cell shape extraction and classification for 3D time-lapse sequences of living cells, based on the SPherical HARMonics transform (SPHARM). Starting from an initial segmentation of the cell surface over time, this mathematical representation enables us to represent each extracted surface by a unique set of coefficients, while taking into account invariance properties such as translation or orientation. Then, unsupervised classification is conducted using a multi-class K-Means approach, so as to extract the most pertinent number of classes representing the different phases of the cell deformation. Experimental results on several sequences give encouraging results, and show that the proposed approach can be used to perform automated sequence annotation, and can be further applied to compare shape characteristics across different cell populations.**

I. Introduction

Cell deformation is central to several fundamental biological processes, many of which have important medical implications. For instance, cells of a developing embryo migrate to distant locations, where they specialize in shape and in function on the onset of organ morphogenesis [8]. More generally, cells and unicellular organisms characterized by amoeboid motion exhibit an ordered cycle of complex shape changes in order to generate movement [1]. Understanding the mechanisms and factors impacting on cellular shape is thus a crucial aspect in cell biology, and calls for shape quantification tools able to efficiently describe and further discriminate the variety of shape configurations.

A wealth of generic shape descriptors have been proposed in the literature over the past years. Simple descriptors include basic measures such as size or sphericity, while morphological descriptors exploit a voxelized representation of the object to compute skeletons and other geodesic features from the object. Such descriptors are simple and intuitive, yet they only provide an approximate description of the shape at hand, moreover they are particularly sensitive to small shape variabilities. To overcome these issues, more advanced mathematical descriptors based on frequency analysis have been developed, and aim to represent the surface of a given object as a combination of basis mathematical functions. In this category, the SPherical HARMonics transform (SPHARM) has received extensive attention over the past decade, with multiple application in biological shape modeling or comparison [7], [9]. The SPHARM transform considers any closed shape as a function of the unit sphere, and simplifies this function into a unique set of coefficients, facilitating subsequent shape characterization and classification tasks. They are particularly well suited for shape sets which exhibit important shape variabilities such as living cells, and offer interesting properties such as position and orientation invariance.

In this paper, we propose a novel application of the SPHARM transform to perform automatic quantification and unsupervised classification of cell shape in 3D+t microscopy sequences. The cell shapes are initially extracted (segmented) from the original stacks using our 3D Active Mesh framework, which describes each cell surface using a triangular mesh surface of adjustable resolution (we refer the reader to [4] for details). Then, each mesh is projected onto the unit sphere (cf. section II-A) and then transformed into the spherical harmonics space (cf. section II-B) for subsequent shape analysis and classification using an unsupervized K-Means approach (cf. section III). Preliminary results show that several shape configurations can be automatically distinguished during the cell deformation over time, allowing automatic annotation of 3D time-lapse sequences. Finally, we conclude in section IV by discussing the potential applications of this work for cell shape recognition in biological sequences.

II. Shape description using Spherical Harmonics

The spherical harmonics transform applies to scalar or vector-valued functions of the unit sphere $f : S^2 \longmapsto \mathbb{R}^N$. Hence, the first step in the analysis is to perform a one-to-one mapping of the cell surface onto the unit sphere. Bijectivity ensures unicity of the analysis and allows to reconstruct the original surface from its spherical projection.

A. Spherical surface mapping and parameterization

Spherical surface mapping has received substantial attention from the computer vision community, for the numerous application in computer graphics, object modeling and shape analysis [3]. Spherical surface mapping is another member of the family of inverse problems, which must be solved iteratively, while suitable regularization strategies should

All authors are with the Institut Pasteur, Quantitative Image Analysis Unit, 25 rue du Dr. Roux, F-75015 Paris, France, and with the CNRS URA 2582, 25 rue du Dr. Roux, F-75015 Paris, France (email: {cducroz,jcolivo,adufour}@pasteur.fr).

This work was funded by Institut Pasteur.

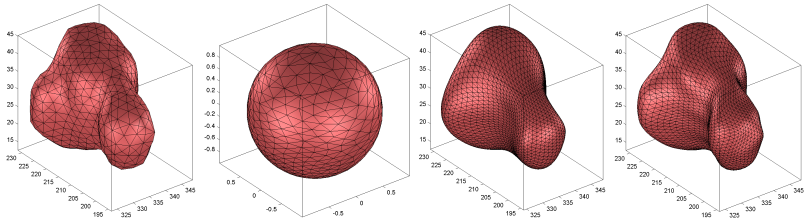

Fig. 1. Surface mapping and reconstruction using the SPHARM-MAT toolbox. (a) Original surface; (b) Mapping on the unit-sphere; (c,d) Reconstructed surface using $l = 5$ (c) and $l = 11$ (d).

be employed to minimize surface distortion and converge toward a unique bijective mapping.

While earlier approaches relied on a voxelized representation of the object surface [2], more recent techniques have allowed to map arbitrary triangular meshes, e.g. [5], [10]. In this work we use the CALD framework [10], which has the advantage of measuring a mapping quality criterion, and produces parameterized surfaces that are directly amenable to SPHARM transform, as we shall describe later.

Like many other mapping techniques, a North and South pole must be chosen on the surface to initialize the mapping process. In the CALD approach, these poles are chosen as the two vertices with the most distant projection onto the principal shape axis. Then, the algorithm performs an iterative mapping that controls area and length distortions simultaneously. This is done by applying a local and a global smoothing alternatively. Local smoothing is achieved by minimizing the area distortion cost locally for each mesh vertex, i.e. by moving each vertex such that all triangles in the immediate neighborhood have equal area. The global smoothing aims to equalize the area distortion cost for all the mesh vertices, by setting the North Pole towards the most distorted vertex thanks to a rotation. This step rearranges the parameter space so that every spherical region is converted to a new region with same area as the corresponding region on the object surface. In practice, global smoothing does not control length distortion, therefore the algorithm alternate between local and global smoothing until convergence. An illustration of the surface mapping is given in Fig. 1-b.

B. The Spherical Harmonics Transform

SPherical HARMonic (thereafter SPHARM) analysis is generally seen as the extension of Fourier analysis on the unit sphere. In the same way that vectors can be described through projections onto each axis (i.e. by scalar products), expansion coefficients (scalar product between functions) can be used to describe functions. On the unit sphere, an orthonormal basis for the Hilbert space of square-integrable function is given by the spherical harmonics:

$$Y_l^m(\theta,\varphi) = k_{l,m} P_l^m(\cos\theta) e^{im\varphi}, \tag{1}$$

where l and m are respectively the degree and order of the harmonic, $k_{l,m}$ is the expansion coefficient and P_l^m is the associated Legendre polynomial. Using this basis, any spherical scalar function $f(\theta,\varphi)$ can be expanded as follows:

$$f(\theta,\varphi) = \sum_{l=0}^{\infty} \sum_{m=-l}^{l} \hat{f}(l,m) Y_l^m(\theta,\varphi), \tag{2}$$

where $\hat{f}(l,m)$ is the (l,m) harmonic coefficient, given by:

$$\hat{f}(l,m) = k_{l,m} \int_0^{\pi} \int_0^{2\pi} e^{-im\varphi} f(\theta,\varphi) P_l^m(\cos\theta) \sin\theta d\varphi d\theta \tag{3}$$

The coefficients $\hat{f}(l,m)$ (3) are unique, thus they can be used directly to describe any arbitrary shape. The spectral decomposition of the input signal is then straightforward: lower degrees correspond to lower frequencies and hence describe the global shape of the object, while higher degrees describe the details of the surface.

Higher dimensional (non-scalar) spherical functions can also be expanded using SPHARM, by expanding each component of the function independently. In this work, the transform is applied to a surface defined in the Cartesian space (x,y,z) and parameterized into a spherical signal written in the polar system as $\mathbf{v}(\theta,\varphi) = (x(\theta,\varphi)\, y(\theta,\varphi)\, z(\theta,\varphi))^T$. Hence when (θ,φ) runs over the sphere, $\mathbf{v}(\theta,\varphi)$ runs over the object surface. The SPAHRM transform is then applied to each component of $\mathbf{v}(\theta,\varphi)$ independently, yielding SPHARM coefficients with three components.

An appealing property of the SPHARM transform is that a rotation in the parameter space induces a rotation in the object space. This property allows to compute descriptors that are invariant to rotation [6], thus allowing generalized shape comparison and classification.

III. Application to Cell Shape Classification

We present here experimental results of shape extraction and classification applied to 3D+t video sequences of deforming biological objects observed in 3D fluorescence microscopy. Our experimental model is the parasite *entamoeba histolytica*, a unicellular organism characterized by amoeboid motion. The goal here is to understand the evolution of the various shape configurations adopted by the parasite during its deformation over time.

A. Image acquisition and segmentation

Parasites deform freely within a 3D matrix, and 3D image stacks are acquired every 8 seconds for about 12 to 15 minutes (yielding 10 sequences with 90 to 120 stacks) using a spinning disk confocal microscope equipped with a

25× objective. Automatic segmentation and tracking is then achieved using active meshes [4], providing a precise description of the surface using a triangular mesh that is directly amenable to shape analysis using spherical harmonics.

B. Extraction of the SPHARM coefficients

We use the SPHARM-MAT Toolbox (available at http://www.iupui.edu/∼shenlab) to perform the spherical parameterization and compute the spherical harmonic decomposition (cf. Fig. 1). Rotational invariant descriptors are computed for each shape following [6]:

$$C_{\text{inv}} = \left(C_x^2 + C_y^2 + C_z^2\right)^{1/2} \tag{4}$$

C. Shape classification

Our goal is to perform automated annotation of cell deformation, yet with no prior knowledge on the nature of the deformation process. Therefore, we perform unsupervized classification of the harmonic coefficients using the K-Means algorithm, for which we compute an optimal number of classes under the following conditions:

1) Minimize the total number of classes n, to avoid oversegmentation of the shape space,

2) Maximize the distance between classes d_{bc}, given as the squared mean distance between all class centroids μ_n and the center of the shape space $\mu_{\mathcal{S}}$:

$$d_{bc} = \sum_{i=1}^{n} \text{card}(n)(\mu_n - \mu_{\mathcal{S}})^2,$$

3) Minimize the distance within classes d_{wc}, given as the squared mean distance of all shapes to their class centroid:

$$d_{wc} = \sum_{i=1}^{n} \sum_{s \in \mathcal{S}} (s - \mu_{K(s)})^2,$$

where s is an individual of the shape space, and $K(s)$ its corresponding class. A minimal shape dispersion is preferred to assess the significance of each extracted class.

Consequently, we compute the optimal number of classes as $\arg\min_n c(n)$, with $c(n)$ given by:

$$c(n) = \frac{n * d_{wc}}{d_{bc}}.$$

Finally, to cope for the sensitivity of the K-means algorithm to initialization, this criterion is computed for 300 successive classifications initialized randomly, and the best criterion value is kept for each class.

D. Results and discussion

1) Shape clustering: Fig. 2 plots the optimal classification criteria depending on the number of classes. Strikingly, we notice a local minumum around 5 classes for all the analyzed sequences, with 4 and 6 classes also showing good results. As visual assessment, Fig. 4 illustrates the classification on a sequence of 92 time points using 4, 5 and 6 classes, and display for each class the closest cell to the class center. Here we notice that the three first classes are always represented by the same shapes, so is the 4th class in the 5-class and 6-class case. Additionally, we see that class 4 in the 4-class case coincides with class 5 in the 6-class case, suggesting a more ambiguous shape distinction in classes over 3.

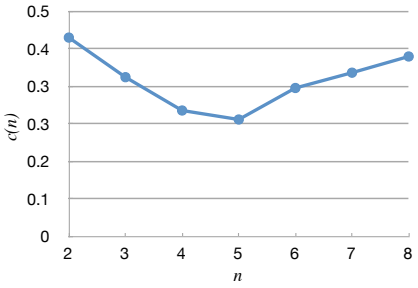

Fig. 2. Evolution of the classification criterion $c(n)$ (Y-axis) for various number of K-Means classes (X-axis). For each class, 300 classification trials are conducted, and the best criterion is kept.

2) Time-based analysis: Fig. 3 illustrates the evolution over time of the first coefficient for the previous cell in the optimal 5-class case, with each value pseudo-colored by its corresponding class. This plot confirms that the first three classes are better distinguished than the others, due to less ambiguity in the classification process. Moreover, we observe that consecutive sequence time-points are generally found in the same classes, demonstrating that small variations in cell shape induce small variations in the spherical harmonic coefficients. This observation suggests that the proposed approach may provide a powerful sequence annotation tool for subsequent human interpretation of the observed dynamics.

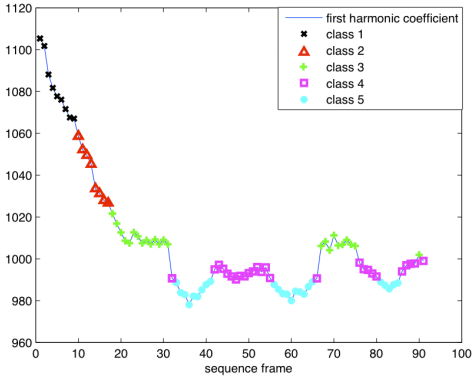

Fig. 3. Evolution of the first harmonic coefficient (Y-axis) along the sequence (X-axis represents sequence frames) for $n = 5$ classes.

3) Discussion: Our results were obtained using the K-Means algorithm with classical euclidean distance measure. In order to verify that this distance measure did not induce a bias due to the variety in scale of the SPHARM coefficients, we performed a PCA analysis of the coefficient space, and found that the highest component retained only 21% of the information, showing that the information is quite homogeneously distributed. This distribution may strongly depend on the application, therefore this distance measure should be adjusted accordingly.

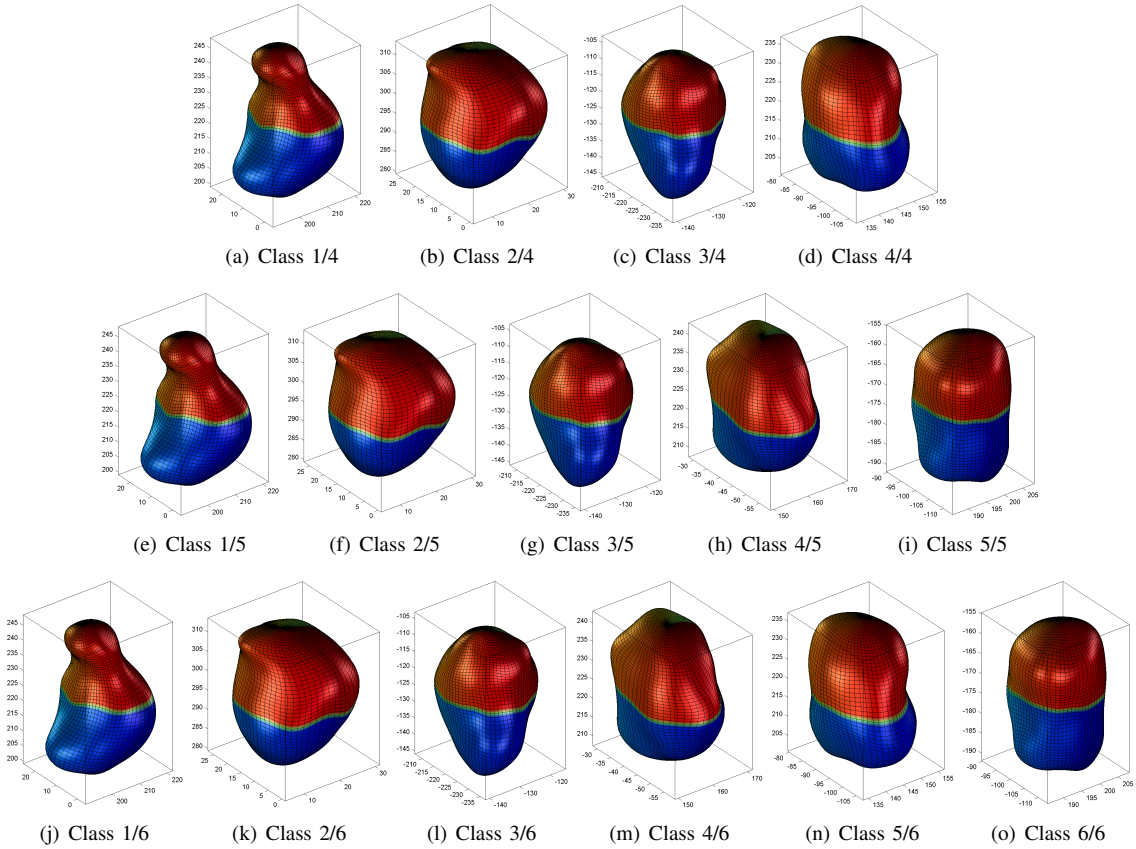

(a) Class 1/4 (b) Class 2/4 (c) Class 3/4 (d) Class 4/4

(e) Class 1/5 (f) Class 2/5 (g) Class 3/5 (h) Class 4/5 (i) Class 5/5

(j) Class 1/6 (k) Class 2/6 (l) Class 3/6 (m) Class 4/6 (n) Class 5/6 (o) Class 6/6

Fig. 4. Unsupervised classification of harmonic surfaces with varying number of classes. For each class, the closest surface to the class center is displayed.

IV. Conclusion

We have presented a novel application of the Spherical Harmonics transform for robust description of cell shape during deformation, enabling unsupervised shape classification for shape recognition and sequence annotation in 3D time-lapse microscopy. The proposed approach represents each cell shape using a unique set of harmonic coefficients which are invariant to position and orientation, allowing to considerably reduce the parameter space and thereby enhance the classification process. Preliminary results on trial data sets are very encouraging, and show that distinct families of shape configurations can be automatically extracted over time, while statistical measures assess the quality of the extracted classes. Further applications of this tool include the computation of differential statistics across different cell populations, for instance in order to assess the impact of the experimental conditions (substrate, environment, chemical compounds) on the cell deformation.

V. Acknowledgements

The authors gratefully acknowledge R. Thibeaux, E. Labruyère and N, Guillén (Institut Pasteur, Cell Biology of Parasitism Unit) for providing the biological material and the time-lapse imaging data.

References

[1] R. Ananthakrishnan, and A. Ehrlicher, "The forces behind cell movement", *Int. J Biol Sci.*, vol. 3, no. 5, 2007, pp. 303-317.

[2] C. Brechbuhler, G. Gerig, and O. Kubler, "Parametrization of Closed Surfaces for 3-D Shape Description", *Computer Vision and Image Understanding*, vol. 61, no. 2, 1995, pp. 154-170.

[3] M. Floater, and K. Hormann, "Surface parameterizations: a tutorial and survey", *in Advances in Multiresolution for Geometric Modelling*, N.A. Dodgson, M.S. Floater and M. A. Sabin, Eds., Springer-Verlag, 2004, pp. 157-186.

[4] A. Dufour, R. Thibeaux, E. Labruyère, N. Guillén, and J.-C. Olivo-Marin, "3D Active Meshes: fast discrete deformable models for cell tracking in 3D time-lapse microscopy", *IEEE Transactions on Image Processing*, in press.

[5] X. Gu, and Y. Wang, and T.F. Chan, and P.M. Thompson, and S.T. Yau, "Genus zero surface conformal mapping and its application to brain surface mapping", *IEEE Transactions on Medical Imaging*, vol. 23, no. 8, 2004, pp. 949-958.

[6] M. Kazhdan, and T. Funkhouser, and S. Rusinkiewicz, "Rotation invariant spherical harmonic representation of 3D shape descriptors", *in Eurographics Symposium on Geometry Processing*, 2003.

[7] K. Khairy, J. Foo, and J. Howard, "Shapes of Red Blood Cells: Comparison of 3D Confocal Images with the Bilayer-couple Model", *Cell. and Mol. Bioeng.*, vol. 1, 2008, pp. 173-181.

[8] R. McBeath, D.M. Pirone, C.M. Nelson, K. Bhadriraju, and C.S. Chen, "Cell shape, cytoskeletal tension, and RhoA regulate stem cell lineage commitment", *Develop. Cell*, vol. 6, no. 4, 2004, pp. 483495.

[9] D.W. Ritchie, and G.J.L. Kemp, "Fast Computation, Rotation and Comparison of Low Resolution Spherical Harmonic Molecular Surfaces", *J. Comp. Chemistry*, vol. 20, no. 4, 1999, pp. 383-395.

[10] L. Shen, and F. Makedon, "Spherical mapping for processing of 3D closed surfaces", *Image and Vision Computing*, vol. 24, no. 7, 2006, pp. 743-761.